

1 **Estimating flood quantiles at ungauged sites using nonparametric** 2 **regression methods with spatial components**

3 Martin Durocher^{1,*}, Donald H. Burn¹, Shabnam Mostofi Zadeh¹ and Fahim Ashkar².

4
5 1 - University of Waterloo, Department of Civil and Environmental Engineering, Waterloo (ON),
6 Canada, N2L 3G1.

7 2 - University of Moncton, Department of Mathematics and Statistics, Moncton (NB), Canada,
8 E1A 3E9

9 * - Corresponding author: mduroche@uwaterloo.ca

10

11 **Abstract**

12 Prediction of flood quantiles at ungauged sites has been investigated using several nonparametric
13 regression methods including: local regression based on regions of influence, neural networks and
14 generalized additive models (GAM). These methods were used to describe the relationship
15 between run-off variables and catchment descriptors to predict flood quantiles. Previous work
16 reported the presence of spatial correlation in the residuals for these models. To this end, this study
17 proposes and investigates ways of incorporating spatial components. An L-moments regression
18 technique (LRT) is developed to predict L-moments of target sites and flood quantiles are derived
19 by aggregating quantiles from multiple candidate distributions. The predictive power of the
20 proposed methods is evaluated on a large database of Canadian rivers using cross-validation. The
21 results are examined inside different provinces and hydrological regions to assess the behaviour
22 of the methods. The results show that GAM and local regression using respectively thin plate
23 spline and kriging provide the best predictive powers among the considered methods. Additionally,

24 the LRT method is found to improve prediction power over the well-known index-flood model
25 and has similar results to quantile regression techniques (QRT) when using the same
26 nonparametric regression approaches.

27 **Keywords: Kriging, Flood, Frequency analysis, Generalized additive models, Region of**
28 **influence, Ungauged site, Canada.**

29 **1. Introduction**

30 Estimating the statistical distribution of extreme events is a crucial task in designing safe and cost-
31 efficient infrastructure. For a given catchment, the amount of streamflow data may not be sufficient
32 to carry out a proper at-site frequency analysis with the desired level of accuracy. In such a
33 situation, regional frequency analysis is commonly used to improve the quality of the estimates by
34 transferring additional information from nearby catchments with similar characteristics. In
35 particular, when a target site is ungauged, flood quantiles associated with a given return period
36 must be deduced from the relationship with existing catchment descriptors. Quantile regression
37 technique (QRT) (Thomas and Benson, 1975) is an approach where the model is directly linking
38 the at-site flood quantiles to the catchment descriptors. This method avoids the subjective task of
39 selecting a best distribution at the site of interest, which impacts the extrapolation for longer return
40 periods. However, this approach may lead to incoherent estimations among different return periods
41 as separate models are necessary for every desired return period. Alternatively, parameter
42 regression techniques (PRT) can be used to link the parameters of a target distribution to its
43 catchment descriptors. In terms of performance for estimating flood quantiles at ungauged sites,
44 recent comparison studies concluded that both techniques led to similar results and that the choice

45 between the two methods depends mostly on practical considerations (Ahn and Palmer, 2016;
46 Haddad and Rahman, 2012).

47 Among existing parameter regression techniques, the index-flood method (Hosking and Wallis,
48 1997) is commonly used to estimate flood quantiles based on the assumption that inside a
49 homogenous region all sites follow the same distribution up to a scale factor, called the index-
50 flood. In particular, a neighborhood defines a homogenous region that is unique to a target site and
51 where the pooled catchments are the nearest catchments according to a given metric (Acreman and
52 Sinclair, 1986). Several comparative studies showed that this type of region, commonly called
53 Region Of Influence (ROI), outperforms the use of fixed regions derived from common clustering
54 techniques (Burn, 1990; GREHYS, 1996; Tasker et al., 1996). For gauged-site analysis, the notion
55 of homogeneity of a region is crucial to the validity of the model. For that purpose, the degree of
56 homogeneity is generally evaluated according to statistics comparing the properties of the flood
57 responses (Burn, 1997; Castellarin et al., 2008; Requena et al., 2017; Viglione et al., 2007). When
58 there are no streamflow data, the degree of homogeneity of a region in regards of the target site
59 cannot be directly assessed. However, useful regions can still be delineated using geographical
60 distance or similarity between catchment descriptors (Eng et al., 2007; Zrinji and Burn, 1994),
61 even though the resulting regions may lack hydrological similarities (Burn et al., 1997; Oudin et
62 al., 2010). Nonetheless, the delicate task of delineating and validating homogenous regions can be
63 avoided if one assumes instead that the catchment attributes evolve smoothly inside the descriptor
64 space (Chokmani and Ouarda, 2004; Laio et al., 2011).

65 Linear regression equations are frequently employed to characterize the relationship between run-
66 off variables and catchment descriptors (Pandey and Nguyen, 1999). When the number of gauged
67 sites is limited, the lack of information may prevent the utilization of more complex models, but
68 in general, a nonlinear relationship should be expected (Wittenberg, 1999). Nonparametric
69 regression is a general term associated with various methods for which the relationship between a
70 response variable and some explanatory variables is sufficiently flexible to accommodate for
71 arbitrary patterns, if sufficient information is available. Therefore, the use of nonparametric
72 regression methods for the prediction of a flood quantile at ungauged sites can avoid the formation
73 and validation of homogenous regions by providing a single model valid for all considered
74 catchments.

75 Local regression is one example of nonparametric regression methods where a low-degree
76 polynomial is fitted inside small neighborhoods to locally approximate the global pattern (Altman,
77 1992; Cleveland and Devlin, 1988). This strategy is well known in regional flood frequency
78 analysis as it includes as a special case the utilization of multiple regression inside a region of
79 influence. Another example of a nonparametric regression method is a Neural Network (NN) that
80 is inspired by the way neurons are mapped inside the human brain. For prediction at ungauged
81 sites, neural networks were found to outperform the use of linear models inside homogenous
82 regions in different contexts (Aziz et al., 2014; Dawson et al., 2006; Shu and Burn, 2004; Shu and
83 Ouarda, 2007). Apart from these two better known methods, other nonparametric regression
84 methods investigated in regional frequency analysis include regression trees (Laaha and Blöschl,
85 2006; Schnier and Cai, 2014), support-vector regression (Gizaw and Gan, 2016) and Generalized
86 Additive Models (GAM) (Latraverse et al., 2002; Rahman et al., 2018).

87 Catchment descriptors used as explanatory variables in a regression model can be classified in two
88 groups. One is composed of catchment attributes that are specific to a given location on a river.
89 This group includes, among others, drainage area, channel length and mean slope. The second
90 group represents physio-climatic attributes that are continuous in space, such as rainfall,
91 temperature, forest canopy and soil characteristics. In the United Kingdom, the study of Kjeldsen
92 and Jones (2009) showed that even when this second group of descriptors is used in a regression
93 model, spatial correlation may still be found in the residuals, which indicates that the information
94 passed to the models does not fully characterize the flood-generating process. In particular,
95 gathering information on the underground characteristics can be a major challenge (Oudin et al.,
96 2008). In such case, spatial proximity can be used as a surrogate and several strategies have been
97 considered to efficiently combine information derived from catchment descriptors and spatial
98 proximity. Oudin et al. (2008) in France and Steinschneider et al. (2015) in the United States
99 integrated spatially autocorrelated errors in their regression models. Similarly, Archfield et al.
100 (2013) compared kriging techniques (Castiglioni et al., 2009; Skøien and Blöschl, 2007) in the
101 United States and found that a two-step procedure that performs kriging in the descriptor space
102 followed by kriging of the residuals in geographical space works better than both techniques taken
103 separately.

104 The main objective of the present study is to investigate strategies that can improve the treating of
105 geographical information inside nonparametric regression models for the objective of predicting
106 flood quantiles at ungauged sites. A special interest is given to local regression, which is largely
107 applied in practice, and GAM modelling. The latter possesses a practical mathematical
108 representation and provides straightforward interpretation of the catchment descriptors (Chebana

109 et al., 2014). Due to its practical form, GAM can be directly combined with kriging techniques
110 without requiring a two-step procedure as in the suggestion of Archfield et al. (2013).
111 Alternatively, thin plate splines (TPS) (Green and Silverman, 1993) are a nonparametric regression
112 technique that is specifically designed to model spatial data and Wood (2003) introduced an
113 efficient way of incorporating TPS in GAM modelling. These two approaches extended the class
114 of GAM models by adding a spatial component in a manner that has not been investigated in the
115 context of flood frequency analysis. Similar extensions are also developed for local regression. In
116 this study, these two regression approaches are compared together, and with neural networks, to
117 identify which combinations of nonparametric regression methods and spatial components should
118 be recommended.

119 This study also pursues secondary objectives. In Canada, water policies fall under provincial
120 jurisdiction and for this reason Canadian studies have traditionally been performed at the
121 provincial level (El-Jabi et al., 2016; GREHYS, 1996; Sandrock et al., 1992), even though
122 administrative boundaries are derived for political reasons and do not often have hydrological
123 relevance. Recent studies have illustrated the interest of performing regional frequency analysis at
124 national and even global scale to take advantage of the increasing amount of information and to
125 assess the model performance in different conditions (Durocher et al., 2018; Salinas et al., 2014;
126 Smith et al., 2015). In particular, Canada has diverse climatic and hydrological environments that
127 result in different types of flood regimes (Burn et al., 2016; Buttle et al., 2016). Therefore, the
128 present study considers a large dataset of 770 hydrometric stations across Canada, to investigate
129 how the considered methods perform in different hydrological environments.

130 The present methodology will be denoted L-moment regression technique (LRT) as the L-
131 moments of ungauged sites are predicted on the basis of catchment descriptors (Laio et al., 2011).
132 This strategy can be seen as a special case of parameter regression technique, but where catchments
133 with different distributions can be mixed together and aggregated to compute flood quantiles from
134 multiple candidate distributions. In this framework, the application of GAM is similar to that of
135 GAM location-scale-shape (GAMLSS) (Rigby and Stasinopoulos, 2005), that was used in flood
136 frequency analysis to model nonstationarity in time series (López and Francés, 2013; Villarini et
137 al., 2009). However, the present study focuses on prediction at ungauged sites and develops
138 particular strategies for extending this basic framework for incorporating spatial components and
139 mixing at-site distributions. In particular, a new weighting procedure is investigated for evaluating
140 the relative contribution of each candidate distribution. The proposed method will be compared to
141 the index-flood model and quantile regression techniques to determine which of these three
142 approaches is best.

143 The paper is organized as follows. In section 2, the proposed methodology, including kriging and
144 nonparametric regression, is presented. In section 3, the investigated methods are applied and
145 compared on a large dataset of Canadian rivers. Finally, discussion and general conclusions are
146 provided in Section 4.

147 **2. Methodology**

148 The general methodology consists in fitting separate nonparametric regression models to the first
149 three L-moments of the annual maxima of a river discharge. More precisely, the sample mean
150 (L1), the L-coefficient of variation (LCV), and the L-coefficient of skewness (LSK) are selected.

151 A logarithm transformation is applied to the first two L-moments to obtain more normal-shape
 152 distributions and to enforce positive values. The L-moments are then used to estimate the flood
 153 quantiles of ungauged sites for multiple candidate distributions and a final prediction is obtained
 154 by averaging the output of each candidate. This section starts by presenting the nonparametric
 155 regression methods and continues by describing the procedure to estimate the flood quantiles from
 156 the L-moments predicted at target sites. At the end of the section, criteria are proposed for assessing
 157 the quality of estimated flood quantiles.

158 *2.1 Universal kriging estimator*

159 Kriging is a powerful geostatistical technique for predicting a variable at unknown location s_0
 160 when data are generated by a Gaussian random field. In the present context, kriging can be used
 161 to obtain L-moments at ungauged sites. Let's consider a set of gauged sites $\mathbf{s} = (s_1, \dots, s_n)$ with a
 162 matrix of descriptors $\mathbf{X}(\mathbf{s})$ and a vector of descriptors $\mathbf{x}(s_0)$ at the ungauged site. Similarly, note
 163 $\mathbf{z}(\mathbf{s})$ the vector of the sample L-moment of a specific order. According to this notation, the kriging
 164 model is written

$$165 \quad (1) \quad \begin{aligned} \mathbf{z}(\mathbf{s}) &= \mathbf{X}(\mathbf{s})\boldsymbol{\beta} + \boldsymbol{\varepsilon}(\mathbf{s}), \\ z(s_0) &= \mathbf{x}(s_0)' \boldsymbol{\beta} + \varepsilon(s_0) \end{aligned}$$

166 where $\boldsymbol{\varepsilon} \sim N(0, \boldsymbol{\Sigma})$ is an error term and $\boldsymbol{\beta}$ is a set of parameters. For this kriging model, the
 167 impact of the catchment descriptors is described by the deterministic trend $\mathbf{x}(s_0)' \boldsymbol{\beta}$ and the spatial
 168 component is characterized by the covariance matrix $\boldsymbol{\Sigma}$ of the error terms. This separation
 169 provides a coherent and distinct decomposition of the model influences.

170 The objective of kriging is to predict $\hat{z}(s_0) = \mathbf{a}'\mathbf{z}(\mathbf{s})$ as a linear combination of observed values.
 171 The kriging estimator is obtained by finding the kriging weights \mathbf{a} that minimize the predicting
 172 variance. If the error term follows a known covariance model, then it is possible to compute the
 173 covariance $\sigma = \text{Cov}\{z(s_0), \mathbf{z}(\mathbf{s})\}$ between the gauged and target sites and the variance
 174 $\sigma_0 = \text{Var}\{z(s_0)\}$ at the target site. Under these conditions, the universal kriging predictor has the
 175 form

$$176 \quad (2) \quad \mathbf{a}'\mathbf{z}(\mathbf{s}) = x(s_0)' \hat{\beta} + \sigma' \Sigma^{-1} \{ \mathbf{z}(\mathbf{s}) - \mathbf{X}(\mathbf{s}) \hat{\beta} \},$$

177 where $\hat{\beta} = \{ \mathbf{X}(\mathbf{s})' \Sigma^{-1} \mathbf{X}(\mathbf{s}) \}^{-1} \mathbf{X}(\mathbf{s})' \mathbf{z}(\mathbf{s})$ is the generalized least square estimator (Schabenberger
 178 and Gotway, 2004). In simple words, the universal kriging estimator is the sum of a trend and
 179 corrected residuals derived from the spatial covariance structure. In practice, the covariance matrix
 180 Σ is not known and must be estimated. To this end, a semivariogram model representing the
 181 strength of the covariance as a function of distance can be fitted. See for instance Schabenberger
 182 and Gotway (2004).

183 ***2.2 Generalized additive models***

184 Nonparametric regression models assume that the relationship between the response variable and
 185 explanatory variables is characterized by arbitrary, but continuous functions. For a regression
 186 model with a single explanatory variable the estimated function is chosen from flexible classes,
 187 such as kernel smoothers, spline polynomials or radial basis function (Hastie et al., 2009). One
 188 way to extend nonparametric regression to include several explanatory variables is GAM
 189 modelling. Following the established notation, a GAM trend describing a response variable is

190 (3)
$$z(s) = \mu + \sum_{k=1}^p f_k \{x_k(s)\}$$

191 where μ is the global mean, $\mathbf{x}(s) = \{x_1(s), \dots, x_p(s)\}$ are explanatory variables and f_i are smooth
 192 univariate functions that respect basic conditions that ensure their uniqueness relative to the global
 193 mean (Hastie and Tibshirani, 1986).

194 Spline polynomials are formed as a series of low-order polynomials joined together (under some
 195 regularity conditions) at control points. For well-chosen control points, spline polynomials
 196 represent an attractive modelling strategy that can be assimilated to a linear model. Therefore, a
 197 GAM trend using spline polynomials can be incorporated directly in the kriging model (1).
 198 However, the choice of the control points plays an important role in the quality of the fitting and
 199 using a large number of control points provides more flexibility, but is likely to overfit the data. In
 200 that case, regulation can be used to control the smoothness of the estimated function f_i by adding
 201 further restrictions, or penalties. A common choice is $\int f_k''(t)^2 dt < \lambda_k$ that restrict unnecessary
 202 fluctuations of the second derivative (Green and Silverman, 1993). In practice, different values of
 203 the calibration parameter λ_k are tried and a final model is chosen according to an objective
 204 criterion such as the Generalized Cross-Validation criteria (Craven and Wahba, 1978). However,
 205 adding such regularization falls outside the framework of the universal kriging estimator in
 206 equation (2).

207 The motivation for using the sum of univariate smooth functions in GAM modelling is that the
 208 effect on the response variable with respect to each explanatory variable is straightforward and it

209 was shown that this strategy adapts reasonably well to various nonlinear forms encountered in
210 flood frequency analysis (Chebana et al., 2014). However, that restriction creates limitations. For
211 instance, it means that a GAM model cannot correctly characterize geographical coordinates,
212 because they are treated separately. Consequently, for two or more dimensions, an alternative
213 approach is needed. In this line, for a set of r bivariate control points c_1, \dots, c_r , thin plate spline
214 (TPS) is better suited for modelling spatial data and is defined as a radial basis function

215 (4)
$$f(s) = \sum_{j=1}^r w_j \phi(\|s - c_j\|)$$

216 where $\phi(t) = t^2 \log(t)$. Wood (2003) showed that thin plate splines can be used to expand the
217 capability of GAM models by incorporating a bivariate function that characterizes the interaction
218 between two explanatory variables, while keeping the general interpretability of the GAM model.
219 For predicting L-moments at ungauged sites, a GAM model can be considered where the spatial
220 component is described by thin plate splines. In this case, the deterministic trend includes both the
221 spatial component and the relationship with the catchment descriptors and consequently the error
222 term is assumed to be spatially independent.

223 ***2.3 Other nonparametric regression models***

224 The GAM models described above contain useful strategies for the spatial component in the
225 prediction of L-moments at ungauged sites. Other regression procedures may not share the same
226 mathematical simplicity, but can also lead to accurate predictions. Local regression where a
227 multiple regression model is performed inside a region of influence is one example. In the present
228 study, weights proportional to the distance of a gauged site from the target site are used to give

229 more importance to the closer sites. Formally, if $s_{(i)}$ are the gauged sites of a neighborhood of site
230 $i = 1, \dots, n$, ordered by distance $h_{(i)}$ with the target then the weights are

231 (5)
$$w_{(i)} = 1 - \left(h_{(i)} / h_{(n)} \right)^2.$$

232 Note that only the number of sites in the neighborhood must be calibrated to use the model.
233 Durocher et al. (2018) indicated that using constant neighborhood sizes by hydrological regions
234 can improve the overall quality of the method in comparison to individual calibrations. This
235 recommendation is followed in the present study. Also, as the addition of one site is not likely to
236 bring substantial changes in the fitting, the best calibration is searched among neighborhoods of
237 sizes from 25 to 200 by steps of 5.

238 Although locally linear, the local regression as a whole cannot be treated as a linear model, and
239 therefore the universal kriging estimator (2) with a ROI trend cannot be evaluated. However, a
240 ROI/KRG procedure can be considered by extracting the trend in a first step and then using kriging
241 (or TPS) in a second step to further predict the residuals based on spatial proximity. Here, the mean
242 of the residuals is known to be zero and that assumption is incorporated as a constraint in the
243 simple kriging estimator (Schabenberger and Gotway, 2004). This gives rise to a model having a
244 similar form as the universal kriging estimator, but with a different trend and spatial component.

245 Another alternative to GAM is neural networks (NN). In general, neural networks take different
246 forms, but in the present study, feedforward neural networks with a single hidden layer are
247 considered as they represent a flexible class of models that can approximate any continuous
248 function with the desired precision (Bishop, 1995). The only parameter required for calibration is

249 the number of units or neurons. One challenge with neural networks is that the fitting algorithm
250 often converges to locally optimal solutions. To avoid this behaviour and improve the predictive
251 capability of the model, the neural networks are incorporated in a resampling strategy known as
252 bagging (Hastie et al., 2009; Shu and Burn, 2004). Accordingly, the neural networks are fitted on
253 20 bootstrap samples and the final predictions are taken as the average of the individual outputs.
254 Moreover, Shu and Ouarda (2007) successfully used canonical correlation analysis as a pre-
255 treatment of the explanatory variables to improve the learning rate of a neural network. A similar
256 strategy is adopted here, but with principal component analysis to create standardized and
257 uncorrelated input variables from the catchment descriptors. Finally, the present study investigates
258 the relevance of combining neural network with the kriging (or TPS) of the residuals in a two-step
259 procedure as with local regression.

260 ***2.4 Distributions at target sites***

261 After the prediction of the first three L-moments at a target site, the present methodology follows
262 by estimating the parameters of four candidate distributions. They are the Generalized Extreme
263 Value (GEV), Pearson type III (PE3), Generalized Normal (GNO) and Generalized Logistic
264 (GLO) distributions (Hosking and Wallis, 1997). Similarly to Laio et al. (2011), instead of
265 selecting a single best distribution among the candidates, the final flood quantiles are computed as
266 the average flood quantile of the candidate distributions. However, the present methodology differs
267 as weights are used to represent the relevance of each candidate distribution. These weights are
268 evaluated according to the frequency of each candidate distribution being selected for at-site
269 frequency analysis in the proximity of the target site. The rationale is that if the same distribution
270 is selected for all nearby sites when at-site analyses are performed, it is reasonable to choose the

271 same distribution for the target site. The final weights used for aggregating the flood quantiles are
272 proportional to the sums of the weights w_i in equation (5) for each candidate distribution among
273 the sites in a neighborhood.

274 In context of at-site flood frequency analysis, Zhang et al. (2018) performed a comparison study
275 of several statistical distributions in Canada using several criteria and came to the conclusion that
276 the GEV is generally the best choice for Canadian rivers. Therefore, based on these practical
277 considerations, this methodology intends to select alternative distributions only when this choice
278 is supported by the data. In a first step, the adopted procedure selects the best at-site distribution
279 as the one having the lowest Akaike Information Criterion (AIC) (Di Baldassarre et al., 2009).
280 Afterward, the AIC of the best distribution is compared to the one of the GEV. If they are judged
281 similar, then the GEV is used; otherwise, the best distribution is kept. The present study accepts
282 that two distributions are similar when the difference between their AIC is lower than two. Note
283 that such threshold is not largely biased towards the GEV. In particular, that difference corresponds
284 to the impact of removing one parameter from a nested model; Burnham and Anderson (2002) also
285 suggest that differences greater than 4 should be considered meaningful.

286 An alternative to the presented methodology for evaluating flood quantiles at a target site using L-
287 moments is the index-flood model (IF) using the L-Moment algorithm (Hosking and Wallis, 1997).
288 The index-flood method computes the flood quantile of a site s as $q(s) = z(s) \times q$, where $z(s)$ is
289 the index-flood factor taken here as the mean of the site annual maxima s_i (L1) and q represents
290 the flood quantile of a dimensionless distribution, or regional growth curve. With the L-Moment
291 algorithm, the regional growth curves are estimated using neighborhoods of size 20 and by

292 averaging the LCV and LSK using weights proportional to the record lengths. Hosking and Wallis
293 (1997) reported that neighborhoods of size larger than 20-25 sites do not usually provide more
294 information. Traditionally, the L-Moment algorithm selects a single regional distribution based on
295 a Z-statistic that identifies the distribution having theoretically the most coherent L-kurtosis with
296 the sample. Note that in the present situation, the homogeneity of the regions used for computing
297 the regional growth curve is not verified as it is assumed instead that the L-moments are smoothly
298 evolving in descriptor space.

299 ***2.5 Model evaluation and uncertainty***

300 The assessment of a method for flood frequency analysis is mostly focused on evaluating the
301 capacity of such method in estimating flood quantiles of specific return periods. Leave-one-out
302 cross-validation is often used in that context to evaluate in turn the prediction error made when
303 one site is assumed ungauged. For local regression, such strategy can be efficiently implemented
304 by excluding the target site in each neighborhood. However, for other nonparametric regression
305 methods such as GAM and neural network, refitting a model many times is inefficient.
306 Consequently, k-fold cross-validation is preferred here to limit the computational burden (Hastie
307 et al., 2009). This cross-validation procedure does essentially the same as a leave-one-out cross-
308 validation scheme. In turns, one of k group of sites with similar sizes is considered as ungauged
309 and these sites are predicted by the remaining sites. For the present study $k = 10$ and $n = 770$ sites.
310 Therefore, this strategy reduces by 77 times the number models to be fitted.

311 Based on the residuals of the cross-validation scheme, two criteria are used to evaluate the
312 magnitude of the prediction error. Let $\tilde{z}(s_i)$ be a response variable predicted at the i -th of n sites

313 when considered as ungauged and $z(s_i)$ the observed value. Two well-known criteria are the
 314 Nash-Sutcliffe

315 (6)
$$NSH = 100 \times \left[1 - \frac{\sum_{i=1}^n \{ \tilde{z}(s_i) - z(s_i) \}^2}{\sum_{i=1}^n \left\{ \tilde{z}(s_i) - n^{-1} \sum_{j=1}^n z(s_j) \right\}^2} \right]$$

316 and the mean absolute deviation

317 (7)
$$MAD = n^{-1} \sum_{i=1}^n | \tilde{z}(s_i) - z(s_i) | .$$

318 The NSH criterion provides a measure of the quadratic error relatively to the performance of the
 319 model represented by a global mean. Values close to 100 % indicate good predictive performance.
 320 Alternatively, the MAD criterion is based on absolute errors, which leads to a criterion that is less
 321 affected by large discrepancies and so more robust to potential outliers. Note that the MAD
 322 criterion provides a measurement of the prediction error in the same units as the predicted variable,
 323 while NSH is a dimensionless measure.

324 In general, for two competing methods it is difficult to interpret the meaning of small differences
 325 in performance measures as they can represent either a real gain of prediction skill or be simply
 326 the consequence of random sampling. In the context of hydrological model forecasting, it was
 327 shown that the assessment of significantly better forecasting skills can be determined by hypothesis
 328 testing (DelSole and Tippett, 2014; Hamill, 1999). The same strategy is adopted here to evaluate
 329 prediction skills using the Wilcoxon signed-rank (WSR) test. For the first two predicted L-moments

330 (L1 and LCV), the loss differential of two competing methods with predictions $\tilde{z}(s_i)$ and $\hat{z}(s_i)$ is
331 defined as

$$332 \quad (8) \quad d_i = \log \left\{ \tilde{z}(s_i) / z(s_i) \right\}^2 - \log \left\{ \hat{z}(s_i) / z(s_i) \right\}^2$$

333 and for the L-coefficient of skewness

$$334 \quad (9) \quad d_i = \left\{ \tilde{z}(s_i) - z(s_i) \right\}^2 - \left\{ \hat{z}(s_i) - z(s_i) \right\}^2 .$$

335 The Wilcoxon signed-rank test verifies the hypothesis of a zero-mean rank of the loss differential
336 against a significant (bilateral) difference. Therefore, a small p-value of this test provides evidence
337 that one competing method has superior predictive skills. In particular, as a nonparametric test, the
338 outcome is invariant to the distribution of the loss differential.

339 In the proposed methodology, regression models are fitted directly on the sample L-moments of
340 each site. Consequently, the resulting criteria NSH and MAD do not account for a sampling source
341 of error that could lead to underestimate the true uncertainty of the model (Tasker and Stedinger,
342 1989). Therefore, the fitting of each model is performed on 1000 bootstrap samples to achieve
343 better evaluation of the model uncertainty. In particular, the cross-validation is performed on each
344 bootstrap iteration to obtain reliable measures of the predictive uncertainty. In Canada, to create
345 spatially dependent bootstrap samples, a multivariate Normal copula was found to well represent
346 the strength of the intersite correlation among streamflow data (Durocher et al., 2018). To simulate
347 from the Normal copula, the correlation coefficients of the matrix are deduced from a known power
348 exponential model. The process is repeated to obtain spatially dependent samples inside the

349 uniform interval [0, 1] that are rescaled using the inverse cumulative distribution function
350 estimated from at-site frequency analysis of each site. To compare the level of uncertainty across
351 sites, the coefficient of variation of the estimated flood quantiles is computed and an average
352 coefficient of variation (ACV) is used to describe the overall uncertainty for a specific group of
353 sites.

354 **3. Results**

355 *3.1 Data and hydrological environments*

356 The investigated nonparametric regression methods are applied to a case study of 770 gauged sites
357 in Canada. The hydrometric data were extracted from the Water Survey of Canada (WSC, 2018)
358 and the catchment descriptors were provided by Environment and Climate Change Canada. Every
359 site is verified to have at least 20 years of record with no significant trend according to the Mann-
360 Kendall test. The descriptors considered for the prediction of the L-moments include: drainage
361 area, mean annual precipitation, percentage of watershed covered by waterbodies, stream density,
362 catchments mean slope, site elevation, longitude and latitude. A summary of these descriptors is
363 presented in Table 1. These descriptors were the explanatory variables used by Durocher et al.
364 (2018) for the same database and were selected by cross-validation using local regression.

365 Canada is a vast country with many distinct hydrological environments. To improve the
366 interpretability of the results, the sites are further divided into hydrological regions based on the
367 drainage area and mean annual precipitation. These two catchment attributes were shown to be
368 related to the sample moments of flood distributions (Basu and Srinivas, 2015; Blöschl and

369 Sivapalan, 1997; Meigh et al., 1997). The hydrological regions were formed by hierarchal
370 classification using Ward's method (Ward, 1963) and their total number is determined based on
371 their overall parsimony and interpretability. Figure 1 illustrates the geographical locations of the
372 770 gauged sites regrouped in 7 hydrological regions. Region 1 represents catchments located
373 along the Pacific coast, which receive the largest amount of precipitation in Canada. Regions 2 to
374 4 are wetter catchments mostly found in eastern Canada and in British Columbia, while regions 5
375 to 7 are drier catchments mainly located in the Prairies and northern Canada. One can see that
376 British Columbia is hydrologically diverse as at least one member of every region is found in its
377 territory. Notice also that large watersheds are generally found at the more northerly locations.

378 ***3.2 Regionalization of the L-moments***

379 The quality of the models is assessed by the cross-validation criteria and is reported in Table 2.
380 When no spatial component is included, the GAM method is found to have the least predictive
381 power for the mean (L1) with low NSH and high MAD. This suggests that the assumption of
382 independence between the smooth functions limit the model flexibility. In that regard, ROI offers
383 the best predicting power, with results slightly outperforming NN. Similar observations are made
384 for LCV and LSK. By default, ROI uses the Mahalanobis distance between catchment descriptors
385 to delineate the neighborhood of a target site. Similarly, ROI/GEO is the same method, but using
386 instead the geographical distance. One can see that the change of metric improves the predictive
387 capability of the local regression approach, although based on a WSR test the difference of
388 predictive skills is not significant for L1 and LCV at a significance level of 0.05.

389 Table 2 reveals that the addition of a spatial component (KRG or TPS) increases the accuracy of
390 all nonparametric regression methods. In particular, examining all pairwise comparison with the
391 WSR test, at a significance level of 0.05, leads to the conclusion of superior predictive skill. Based
392 on the MAD criterion, the GAM/TPS method is best for predicting the LCV and GAM/KRG is
393 found to better describe LSK. For L1, the choice of a best approach depends on which cross-
394 validation criteria is examined. This may point toward either GAM/TPS or ROI/KRG. Overall, the
395 difference between methods having both a trend and a spatial component appears relatively small,
396 except for GAM/KRG that does not perform as well as the others for L1. For ROI and NN, kriging
397 appears to do slightly better than TPS. The NSH criterion indicates that L1 and LCV are globally
398 well predicted, with values roughly around 95 and 81 respectively for the best methods. In
399 particular, notice that the NSH value of the GAM method for LCV passes from 70.3 to 81.8 when
400 adding TPS. Similarly, from GAM to GAM/KRG, the NSH criterion for LCV improves by 11.7.
401 These important gains show the importance of geographical proximity in the determination of the
402 scale and shape of the target distribution.

403 ***3.3 Evaluation of the aggregated weights***

404 Section 2.4 described a strategy to use weights for estimating flood quantiles from multiple
405 candidate distributions. For that purpose, the Mahalanobis distance between descriptors was
406 proposed to delineate neighborhoods of size 20. This size of neighborhood was found optimal in
407 terms of cross-validation criteria. Table 3 presents the contingency table of the distributions
408 selected by at-site frequency analysis. As expected, the GEV distribution is preferred in a large
409 proportion (78%). However, Region 5 (smaller and drier) shows a substantial percentage of sites
410 (47%) where the GNO and PE3 distributions are selected. Due to the prevalence of GEV, weights

411 greater than 0.5 are found for that distribution in 84% of the neighborhoods. At the same time, in
412 Region 5 the cumulative weight of the GNO and PE3 is greater than 0.5 in 42% of the cases. This
413 shows that the proposed methodology preserves the specificity of the distribution selected inside
414 hydrological regions. Consequently, in a majority of the sites outside of Region 5, the estimated
415 flood quantiles are essentially those of a GEV distribution, while inside Region 5 a compromise is
416 made between the relevant distributions.

417 *3.4 Estimation of the flood quantiles*

418 In the following, the focus is set on the GAM/TPS and ROI/KRG methods that were found to be
419 the best methods overall for predicting the L-moments at target sites. The cross-validation criteria
420 of the estimated flood quantiles of return period of 10 and 100 years are presented in Table 4.
421 Overall, it is seen that neither of the two methods is systematically superior to the other. Indeed,
422 according to the WSR test, only hydrological region 7 is significantly better modelled by
423 ROI/KRG for a significance level of 0.05. Notice that the NSH of the hydrological regions is
424 always lower than the NSH of all sites, because the predicting errors are compared to the regional
425 means and not the global mean. The hydrological region with the lowest NSH is Region 7 with
426 70.3 for Q100. However, this region has a MAD of 0.293 that is comparable with Region 2 (0.310),
427 even though the latter has a NSH of 84.0. According to MAD, Region 5 (smaller and drier) is the
428 hydrological region estimated with the lowest accuracy.

429 For evaluating the quality of the prediction considering the sampling error, the coefficient of
430 variation of the estimated flood quantiles for each site is evaluated and averaged by hydrological
431 regions. For Q100, apart from Regions 5-6, the average coefficient of variation (ACV) of

432 GAM/TPS is relatively constant between 10% and 12% . The ACV criterion also shows that the
433 flood quantiles in Region 5 are the less accurately predicted with an ACV of almost double that of
434 the others (19.4). The ACV of Q100 for the ROI/KRG model is less constant across hydrological
435 regions (between 8.6 and 13.7), but they are overall slightly lower than those of GAMP/TPS for
436 all sites. For Q10, according to ACV the ROI/KRG method led to more accurate estimates than
437 GAM/TPS, except for Region 2.

438 ***3.5 Comparison of different approaches for computing flood quantiles***

439 Table 5 reports the comparison of different approaches for computing the flood quantiles. The
440 results indicate that the index-flood (IF) method is underperforming when estimating L1 by both
441 GAM/TPS and ROI/KRG. According to the WSR test, the GAM/TPS method using the LRT
442 approach has significantly better prediction skill than the index-flood method to predict Q100 with
443 a p-value less than 0.001. Similar results are observed for ROI/KRG. One reason for this
444 discrepancy is that the index-flood method does not include a spatial component for LCV and
445 LSK, which was shown in Table 2 to provide important information. A second factor could be the
446 choice of the distribution using the Z-statistic. In particular, the adopted procedure for selecting
447 the at-site distribution has chosen the GEV distribution in 78% of the cases, while the GEV
448 distribution is selected in 49% of the neighborhoods using the Z-statistic. To measure the impact
449 of this selection procedure, a variant of the index-flood model (IFW) is considered where the
450 estimated flood quantiles are taken as a weighted average of candidate distributions, like LRT.
451 These results, presented in Table 5, reveal that for Q10 the two variants of the index-flood method
452 are essentially the same in terms of cross-validation criteria, but a slight discrepancy is observed
453 for Q100. This is coherent with the fact that the selection of the regional growth curve has more

454 impact in the extrapolation to the longer return periods and that the averaging approach is more
455 coherent with the at-site selection procedure. However, LRT has also significantly better
456 prediction skill than IFW, according to the WSR test. This shows that the choice of the regional
457 growth curve is not the most important factor to explain the gap in prediction skill between IF and
458 LRT.

459 Previous studies suggested that parameter regression techniques (similar to LRT) have prediction
460 power comparable to quantile regression techniques, QRT (Ahn and Palmer, 2016; Haddad and
461 Rahman, 2012). Table 5 revisits these conclusions and arrives at similar results. In particular,
462 notice that the highest difference in NSH between LRT and QRT is only 0.03, which shows a
463 similar predictive power of these two methods. These findings are also corroborated by the WSR
464 tests with p-values greater than 0.14.

465 The comparison between the various methods have shown overall very similar results in terms of
466 cross-validation when examined at the national level. One reason is that this case study includes a
467 large number of sites and so nonparametric regression methods having comparable features
468 converge to similar solutions. As mentioned, flood frequency analyses in Canada are often
469 performed at the provincial level for political reasons. Therefore, it is useful to investigate the
470 impact of imposing administrative boundaries and limiting the number of sites. The ROI/KRG and
471 the GAM/TPS methods are thus carried out individually for each province. To ensure a minimum
472 of sites by province, the Atlantic provinces (ATL), the three North territories (NT) and Manitoba-
473 Saskatchewan (MS) are pooled together. Also, even though Labrador is part of the Atlantic
474 province of Newfoundland and Labrador, these sites are regrouped with the adjacent province of

475 Quebec (QC). Note that for ROI/KRG, the hydrological regions are not used in this context and a
476 constant neighborhood size is selected for each province. Table 6 shows the cross-validation
477 criteria by “province”, using national and provincial strategies. Overall, the national analysis
478 appears to outperform the provincial analysis when looking at the cross-validation criteria, but for
479 the vast majority of the provinces and for the whole of Canada, the WSR test does not identify a
480 significant difference in prediction skill at a significance level of 0.05. For GAM/TPS, the North
481 territories (NT) and Quebec (QC), having respectively 51 and 58 sites, the cross-validation criteria
482 are clearly greater using the national analysis. At the opposite side, the predictive powers in British
483 Columbia (BC) and Ontario (ON), having respectively 192 and 128 sites, are slightly better when
484 using the provincial analysis. These results suggest that the number of sites in a province may
485 influence the quality of the GAM/TPS outputs. For ROI/KRG, the national analysis also provides
486 slightly more accurate flood quantiles according to NSH and MAD, but the discrepancy between
487 the national and provincial analysis for the northern territories and Quebec are less important.
488 Moreover, the three provinces with most sites (AB, BC and ON) are slightly better predicted by
489 the national analysis. This suggests that ROI/KRG is more stable than GAM/TPS when restricted
490 by administrative boundaries.

491 **4. Conclusions**

492 In this study, nonparametric regression models with spatial components were investigated for
493 predicting flood quantiles at ungauged sites. The proposed methodology used three separate
494 regression models to predict the first three L-moments of a target distribution. The flood quantiles
495 were then computed as a weighted average of the flood quantile derived by multiple candidate

496 distributions and a weighting scheme was developed to represent the relative importance of each
497 distribution in the proximity of the target site. The overall performance of the nonparametric
498 regression methods was evaluated using cross-validation on a case study of 770 sites in Canada.

499 The results were summarized at the national level, but also inside 7 relevant hydrological and 7
500 administrative regions. This allowed verification of how the considered methods behave in
501 different situations. It was shown that all nonparametric regression methods worked best when a
502 spatial component was added. In particular, a GAM model combined with thin plate spline
503 (GAM/TPS) and a local regression model using kriging (ROI/KRG) were shown to provide
504 globally the most accurate flood quantile estimates. Overall, the cross-validation criteria used to
505 compare these two methods did not identify a better method and the WSR tests showed no
506 significant difference in prediction skills among them. Each method was found to perform slightly
507 better than the other depending on the context and criteria examined. This resemblance in terms of
508 predictive power could be attributed to the large number of sites present in this case study, which
509 allowed them to converge toward similar solutions. Dividing the analysis by administrative regions
510 revealed a small reduction in the predictive power, but this reduction was not found significant
511 according to the WSR test. Nonetheless, these restrictions brought about by use of administrative
512 regions appear to have affected the performance of GAM/TPS more than ROI/KRG.

513 Further comparisons showed that the proposed L-moment regression techniques outperform the
514 index-flood method by incorporating spatial information in the L-moments of second and third
515 order. On the other hand, the L-moment regression techniques showed predictive power similar to
516 that of quantile regression techniques. Therefore, without loss of efficiency, the L-moment

517 regression techniques have an interesting capacity of mixing sites with different candidate
518 distributions. Like the quantile regression techniques and parametric regression techniques, it
519 provides coherent estimates of flood quantiles when evaluated for multiples return periods.

520 Globally, GAM/TPS and ROI/KRG could be recommended for performing flood frequency
521 analysis at ungauged sites. The GAM method has the advantage of having more straightforward
522 descriptions of the relationship between the L-moments and the catchment descriptors. On the
523 other hand, because frequency analysis using local regression can be limited to close
524 neighborhoods and administrative boundaries do not greatly affect its predictive power, ROI/KRG
525 may be attractive in practice when only one or few sites are of interest. In particular, this would
526 greatly facilitate the resampling strategy necessary for evaluating model uncertainty affected by
527 sampling error.

528 **Acknowledgement**

529 This work was supported by the Natural Science and Engineering Research Council (NSERC)
530 Canadian FloodNet (# NETGP 451456 – 13). Computation were realized using the R environment
531 (R Core Team, 2017).

532

533 **References**

- 534 Acreman, M., Sinclair, C., 1986. Classification of drainage basins according to their physical
535 characteristics; an application for flood frequency analysis in Scotland. *Journal of*
536 *Hydrology* 84, 365–380.
- 537 Ahn, K.-H., Palmer, R., 2016. Regional flood frequency analysis using spatial proximity and basin
538 characteristics: Quantile regression vs. parameter regression technique. *Journal of*
539 *Hydrology* 540, 515–526. <https://doi.org/10.1016/j.jhydrol.2016.06.047>
- 540 Altman, N.S., 1992. An Introduction to Kernel and Nearest-Neighbor Nonparametric Regression.
541 *The American Statistician* 46, 175–185. <https://doi.org/10.1080/00031305.1992.10475879>
- 542 Archfield, S.A., Pugliese, A., Castellarin, A., Skøien, J.O., Kiang, J.E., 2013. Topological and
543 canonical kriging for design flood prediction in ungauged catchments: an improvement
544 over a traditional regional regression approach? *Hydrol. Earth Syst. Sci.* 17, 1575–1588.
545 <https://doi.org/10.5194/hess-17-1575-2013>
- 546 Aziz, K., Rahman, A., Fang, G., Shrestha, S., 2014. Application of artificial neural networks in
547 regional flood frequency analysis: A case study for Australia. *Stochastic Environmental*
548 *Research and Risk Assessment* 28, 541–554.
- 549 Basu, B., Srinivas, V.V., 2015. A recursive multi-scaling approach to regional flood frequency
550 analysis. *Journal of Hydrology* 529, 373–383.
551 <https://doi.org/10.1016/j.jhydrol.2015.07.037>
- 552 Bishop, C.M., 1995. *Neural networks for pattern recognition*. Oxford university press.
- 553 Blöschl, G., Sivapalan, M., 1997. Process controls on regional flood frequency: Coefficient of
554 variation and basin scale. *Water Resour. Res.* 33, 2967–2980.
555 <https://doi.org/10.1029/97WR00568>
- 556 Burn, D.H., 1997. Catchment similarity for regional flood frequency analysis using seasonality
557 measures. *Journal of Hydrology* 202, 212–230. [https://doi.org/10.1016/S0022-](https://doi.org/10.1016/S0022-1694(97)00068-1)
558 [1694\(97\)00068-1](https://doi.org/10.1016/S0022-1694(97)00068-1)
- 559 Burn, D.H., 1990. An appraisal of the “region of influence” approach to flood frequency analysis.
560 *Hydrological Sciences Journal* 35, 149–165. <https://doi.org/10.1080/02626669009492415>
- 561 Burn, D.H., Whitfield, P.H., Sharif, M., 2016. Identification of changes in floods and flood regimes
562 in Canada using a peaks over threshold approach. *Hydrol. Process.* 30, 3303–3314.
563 <https://doi.org/10.1002/hyp.10861>
- 564 Burn, D.H., Zrinji, Z., Kowalchuk, M., 1997. Regionalization of Catchments for Regional Flood
565 Frequency Analysis. *Journal of Hydrologic Engineering* 2, 76–82.
566 [https://doi.org/10.1061/\(ASCE\)1084-0699\(1997\)2:2\(76\)](https://doi.org/10.1061/(ASCE)1084-0699(1997)2:2(76))
- 567 Burnham, K.P., Anderson, D.R., 2002. *Model Selection and Multimodel Inference: A Practical*
568 *Information-Theoretic Approach*, 2nd ed. Springer-Verlag, New York.

- 569 Buttle, J.M., Allen, D.M., Caissie, D., Davison, B., Hayashi, M., Peters, D.L., Pomeroy, J.W.,
570 Simonovic, S., St-Hilaire, A., Whitfield, P.H., 2016. Flood processes in Canada: Regional
571 and special aspects. *Canadian Water Resources Journal / Revue canadienne des ressources*
572 *hydriques* 41, 7–30. <https://doi.org/10.1080/07011784.2015.1131629>
- 573 Castellarin, A., Burn, D.H., Brath, A., 2008. Homogeneity testing: How homogeneous do
574 heterogeneous cross-correlated regions seem? *Journal of Hydrology* 360, 67–76.
575 <https://doi.org/10.1016/j.jhydrol.2008.07.014>
- 576 Castiglioni, S., Castellarin, A., Montanari, A., 2009. Prediction of low-flow indices in ungauged
577 basins through physiographical space-based interpolation. *Journal of Hydrology* 378, 272–
578 280. <https://doi.org/10.1016/j.jhydrol.2009.09.032>
- 579 Chebana, F., Charron, C., Ouarda, T.B.M.J., Martel, B., 2014. Regional frequency analysis at
580 ungauged sites with the generalized additive model. *Journal of hydrometeorology* 15,
581 2418–2428. <https://doi.org/10.1175/JHM-D-14-0060.1>
- 582 Chokmani, K., Ouarda, T.B.M.J., 2004. Physiographical space-based kriging for regional flood
583 frequency estimation at ungauged sites. *Water Resources Research* 40.
584 <https://doi.org/10.1029/2003WR002983>
- 585 Cleveland, W.S., Devlin, S.J., 1988. Locally Weighted Regression: An Approach to Regression
586 Analysis by Local Fitting. *Journal of the American Statistical Association* 83, 596–610.
587 <https://doi.org/10.2307/2289282>
- 588 Craven, P., Wahba, G., 1978. Smoothing noisy data with spline functions. *Numerische*
589 *Mathematik* 31, 377–403.
- 590 Dawson, C.W., Abraham, R.J., Shamseldin, A.Y., Wilby, R.L., 2006. Flood estimation at ungauged
591 sites using artificial neural networks. *Journal of Hydrology* 319, 391–409.
592 <https://doi.org/10.1016/j.jhydrol.2005.07.032>
- 593 DelSole, T., Tippet, M.K., 2014. Comparing Forecast Skill. *Mon. Wea. Rev.* 142, 4658–4678.
594 <https://doi.org/10.1175/MWR-D-14-00045.1>
- 595 Di Baldassarre, G., Laio, F., Montanari, A., 2009. Design flood estimation using model selection
596 criteria. *Physics and Chemistry of the Earth, Parts A/B/C, Recent developments of*
597 *statistical tools for hydrological application* 34, 606–611.
598 <https://doi.org/10.1016/j.pce.2008.10.066>
- 599 Durocher, M., Burn, D.H., Mostofi Zadeh, S., 2018. A nationwide regional flood frequency
600 analysis at ungauged sites using ROI/GLS with copulas and super regions. *EarthArXiv*.
601 <https://doi.org/10.31223/osf.io/qrnfe>
- 602 El-Jabi, N., Caissie, D., Turkkan, N., 2016. Flood analysis and flood projections under climate
603 change in New Brunswick. *Canadian Water Resources Journal* 41, 319–330.
604 <https://doi.org/10.1080/07011784.2015.1071205>
- 605 Eng, P. C. Milly, Gary D. Tasker, 2007. Flood Regionalization: A Hybrid Geographic and
606 Predictor-Variable Region-of-Influence Regression Method. *Journal of Hydrologic*
607 *Engineering* 12, 585–591. [https://doi.org/10.1061/\(ASCE\)1084-0699\(2007\)12:6\(585\)](https://doi.org/10.1061/(ASCE)1084-0699(2007)12:6(585))

- 608 Gizaw, M.S., Gan, T.Y., 2016. Regional Flood Frequency Analysis using Support Vector
609 Regression under historical and future climate. *Journal of Hydrology* 538, 387–398.
610 <https://doi.org/10.1016/j.jhydrol.2016.04.041>
- 611 Green, P.J., Silverman, B.W., 1993. *Nonparametric regression and generalized linear models: a
612 roughness penalty approach*. Chapman & Hall/CRC.
- 613 GREHYS, 1996. Presentation and review of some methods for regional flood frequency analysis.
614 *Journal of Hydrology* 186, 63–84. [https://doi.org/10.1016/S0022-1694\(96\)03042-9](https://doi.org/10.1016/S0022-1694(96)03042-9)
- 615 Haddad, K., Rahman, A., 2012. Regional flood frequency analysis in eastern Australia: Bayesian
616 GLS regression-based methods within fixed region and ROI framework – Quantile
617 Regression vs. Parameter Regression Technique. *Journal of Hydrology* 430–431, 142–161.
618 <https://doi.org/10.1016/j.jhydrol.2012.02.012>
- 619 Hamill, T.M., 1999. Hypothesis Tests for Evaluating Numerical Precipitation Forecasts. *Wea.
620 Forecasting* 14, 155–167. [https://doi.org/10.1175/1520-
621 0434\(1999\)014<0155:HTFENP>2.0.CO;2](https://doi.org/10.1175/1520-0434(1999)014<0155:HTFENP>2.0.CO;2)
- 622 Hastie, T., Tibshirani, R., 1986. Generalized additive models. *Statistical science* 297–310.
- 623 Hastie, T., Tibshirani, R., Friedman, J.H., 2009. *The elements of statistical learning: data mining,
624 inference, and prediction*, Springer series in statistics. Springer.
- 625 Hosking, J.R.M., Wallis, J.R., 1997. *Regional frequency analysis: an approach based on L-
626 moments*. Cambridge Univ Pr.
- 627 Kjeldsen, T.R., Jones, D.A., 2009. An exploratory analysis of error components in hydrological
628 regression modeling. *Water Resour. Res.* 45, W02407.
629 <https://doi.org/10.1029/2007WR006283>
- 630 Laaha, G., Blöschl, G., 2006. A comparison of low flow regionalisation methods—catchment
631 grouping. *Journal of Hydrology* 323, 193–214.
632 <https://doi.org/10.1016/j.jhydrol.2005.09.001>
- 633 Laio, F., Ganora, D., Claps, P., Galeati, G., 2011. Spatially smooth regional estimation of the flood
634 frequency curve (with uncertainty). *Journal of Hydrology* 408, 67–77.
635 <http://dx.doi.org/10.1016/j.jhydrol.2011.07.022>
- 636 Latraverse, M., Rasmussen, P.F., Bernard, B., 2002. Regional estimation of flood quantiles:
637 Parametric versus nonparametric regression models. *Water Resources Research* 38, 1–1.
638 <https://doi.org/10.1029/2001WR000677>
- 639 López, J., Francés, F., 2013. Non-stationary flood frequency analysis in continental Spanish rivers,
640 using climate and reservoir indices as external covariates. *Hydrol. Earth Syst. Sci.* 17,
641 3189–3203. <https://doi.org/10.5194/hess-17-3189-2013>
- 642 Meigh, J.R., Farquharson, F.A.K., Sutcliffe, J.V., 1997. A worldwide comparison of regional flood
643 estimation methods and climate. *Hydrological Sciences Journal* 42, 225–244.
644 <https://doi.org/10.1080/02626669709492022>

- 645 Oudin, L., Andréassian, V., Perrin, C., Michel, C., Le Moine, N., 2008. Spatial proximity, physical
646 similarity, regression and ungauged catchments: A comparison of regionalization
647 approaches based on 913 French catchments. *Water Resources Research* 44.
648 <https://doi.org/10.1029/2007WR006240>
- 649 Oudin, L., Kay, A., Andréassian, V., Perrin, C., 2010. Are seemingly physically similar catchments
650 truly hydrologically similar? *Water Resources Research* 46, n/a–n/a.
651 <https://doi.org/10.1029/2009WR008887>
- 652 Pandey, G.R., Nguyen, V.-T.-V., 1999. A comparative study of regression based methods in
653 regional flood frequency analysis. *Journal of Hydrology* 225, 92–101.
654 [https://doi.org/10.1016/S0022-1694\(99\)00135-3](https://doi.org/10.1016/S0022-1694(99)00135-3)
- 655 Rahman, A., Charron, C., Ouarda, T.B.M.J., Chebana, F., 2018. Development of regional flood
656 frequency analysis techniques using generalized additive models for Australia. *Stoch
657 Environ Res Risk Assess* 32, 123–139. <https://doi.org/10.1007/s00477-017-1384-1>
- 658 Requena, A.I., Chebana, F., Ouarda, T.B.M.J., 2017. Heterogeneity measures in hydrological
659 frequency analysis: review and new developments. *Hydrol. Earth Syst. Sci.* 21, 1651–1668.
660 <https://doi.org/10.5194/hess-21-1651-2017>
- 661 Rigby, R.A., Stasinopoulos, D.M., 2005. Generalized additive models for location, scale and
662 shape. *Journal of the Royal Statistical Society: Series C (Applied Statistics)* 54, 507–554.
663 <https://doi.org/10.1111/j.1467-9876.2005.00510.x>
- 664 Salinas, J.L., Castellarin, A., Viglione, A., Kohnová, S., Kjeldsen, T.R., 2014. Regional parent
665 flood frequency distributions in Europe – Part 1: Is the GEV model suitable as a pan-
666 European parent? *Hydrol. Earth Syst. Sci.* 18, 4381–4389. <https://doi.org/10.5194/hess-18-4381-2014>
- 668 Sandrock, G., Viraraghavan, T., Fuller, G.A., 1992. Estimation of Peak Flows for Natural
669 Ungauged Watersheds in Southern Saskatchewan. *Canadian Water Resources Journal /
670 Revue canadienne des ressources hydriques* 17, 21–31.
671 <https://doi.org/10.4296/cwrj1701021>
- 672 Schabenberger, O., Gotway, C.A., 2004. *Statistical methods for spatial data analysis*. CRC Press.
- 673 Schnier, S., Cai, X., 2014. Prediction of regional streamflow frequency using model tree
674 ensembles. *Journal of Hydrology* 517, 298–309.
675 <https://doi.org/10.1016/j.jhydrol.2014.05.029>
- 676 Shu, C., Burn, D.H., 2004. Artificial neural network ensembles and their application in pooled
677 flood frequency analysis. *Water Resour. Res.* 40, W09301.
678 <https://doi.org/10.1029/2003WR002816>
- 679 Shu, C., Ouarda, T.B.M.J., 2007. Flood frequency analysis at ungauged sites using artificial neural
680 networks in canonical correlation analysis physiographic space. *Water Resources Research*
681 43. <https://doi.org/10.1029/2006WR005142>
- 682 Skøien, J.O., Blöschl, G., 2007. Spatiotemporal topological kriging of runoff time series. *Water
683 Resources Research* 43, n/a–n/a. <https://doi.org/10.1029/2006WR005760>

- 684 Smith, A., Sampson, C., Bates, P., 2015. Regional flood frequency analysis at the global scale.
685 Water Resources Research 51, 539–553. <https://doi.org/10.1002/2014WR015814>
- 686 Steinschneider, S., Yang, Y.-C.E., Brown, C., 2015. Combining regression and spatial proximity
687 for catchment model regionalization: a comparative study. Hydrological Sciences Journal
688 60, 1026–1043. <https://doi.org/10.1080/02626667.2014.899701>
- 689 Tasker, G., Stedinger, J., 1989. An operational GLS model for hydrologic regression. Journal of
690 Hydrology 111, 361–375. [https://doi.org/10.1016/0022-1694\(89\)90268-0](https://doi.org/10.1016/0022-1694(89)90268-0)
- 691 Tasker, G.D., Hodge, S.A., Barks, C.S., 1996. Region of Influence Regression for Estimating the
692 50-Year Flood at Ungaged Sites1. JAWRA Journal of the American Water Resources
693 Association 32, 163–170. <https://doi.org/10.1111/j.1752-1688.1996.tb03444.x>
- 694 Thomas, D., Benson, M., 1975. Generalization of streamflow characteristics from drainage-basin
695 characteristics. US Geological Survey Water-Supply Paper.
- 696 Viglione, A., Laio, F., Claps, P., 2007. A comparison of homogeneity tests for regional frequency
697 analysis. Water Resour. Res. 43, W03428. <https://doi.org/10.1029/2006WR005095>
- 698 Villarini, G., Serinaldi, F., Smith, J.A., Krajewski, W.F., 2009. On the stationarity of annual flood
699 peaks in the continental United States during the 20th century. Water Resour. Res. 45,
700 W08417. <https://doi.org/10.1029/2008WR007645>
- 701 Ward, J.H., 1963. Hierarchical Grouping to Optimize an Objective Function. Journal of the
702 American Statistical Association 58, 236–244.
703 <https://doi.org/10.1080/01621459.1963.10500845>
- 704 Wittenberg, H., 1999. Baseflow recession and recharge as nonlinear storage processes.
705 Hydrological Processes 13, 715–726. [https://doi.org/10.1002/\(SICI\)1099-
706 1085\(19990415\)13:5<715::AID-HYP775>3.0.CO;2-N](https://doi.org/10.1002/(SICI)1099-1085(19990415)13:5<715::AID-HYP775>3.0.CO;2-N)
- 707 Wood, S.N., 2003. Thin plate regression splines. Journal of the Royal Statistical Society: Series B
708 (Statistical Methodology) 65, 95–114. <https://doi.org/10.1111/1467-9868.00374>
- 709 WSC, 2018. Water Survey of Canada [WWW Document]. URL
710 <http://www.wsc.ec.gc.ca/applications/H2O/index-eng.cfm>
- 711 Zhang, Z., 2018. Identification of a broadly accepted statistical distribution for at-site flood
712 frequency analysis in Canada.
- 713 Zrinji, Z., Burn, D.H., 1994. Flood frequency analysis for ungauged sites using a region of
714 influence approach. Journal of Hydrology 153, 1–21. [https://doi.org/10.1016/0022-
715 1694\(94\)90184-8](https://doi.org/10.1016/0022-1694(94)90184-8)
- 716 Zhang, Z., Stadnyk, T.A., Burn, D.H., 2018. Identification of a broadly accepted statistical
717 distribution for at-site flood frequency analysis in Canada. Presented at the 71rst CWRA
718 National Conference, May 28 – June 1, Victoria, BC, Canada.
- 719

720

721 **Tables**

722 **Table 1: Summary statistics of streamflow data and catchment descriptors.**

Variables	Abrv.	Min	Q1	Med	Avg	Q3	Max
Record length (yr)		20	25	36	39	48	111
mean annual maximum discharge (m³/s)		0.2	13.4	45.6	206.9	174.1	5068.3
Drainage area (km²)	area	1	146	460	2829	1992	48867
Basin mean slope (%)	slope	<0.1	1.2	3.6	10.5	17.1	59.0
Waterbody area (%)	wb	<0.1	0.4	1.3	3.7	4.5	38.3
Stream density (km⁻¹)	dens	<0.1	0.6	1.0	1.2	1.6	3.4
Elevation at site (m)	elev	1	181	382	474	731	1699
Mean annual precipitation (mm)	map	213	498	761	836	1052	3216

723

724

725

726

727 **Table 2: Cross-validation criteria for predicted L-moments.**

Trend	Spatial	NSH			MAD		
		L1	LCV	LSK	L1	LCV	LSK
GAM	(*)	92.5	70.3	28.4	0.370	0.203	0.090
	KRG	93.5	81.0	40.0	0.340	0.158	0.081
	TPS	95.1	81.8	39.3	0.296	0.154	0.082
	KRG	93.5	81.0	40.0	0.340	0.158	0.081
ROI	(*)	94.5	78.1	30.6	0.327	0.172	0.090
	GEO	94.6	79.5	33.6	0.317	0.163	0.086
	KRG	95.2	81.6	36.8	0.300	0.157	0.085
	TPS	95.0	81.2	34.5	0.305	0.158	0.087
NN	(*)	93.9	75.2	28.0	0.337	0.183	0.091
	KRG	95.1	81.6	36.3	0.298	0.156	0.085
	TPS	94.9	81.3	34.2	0.305	0.158	0.087

728 (*) indicates no spatial component is included...

729 **Bold** indicates the best criteria in columns

730

731 **Table 3: Contingency table of the selected at-site distributions for geographical regions**
732 **indicated in Figure 1.**

Region	GEV	GLO	GNO	PE3	Total
1	21	0	0	1	22
2	34	0	0	3	37
3	165	5	1	7	178
4	81	5	1	1	88
5	114	1	27	73	215
6	104	3	5	20	132
7	85	8	1	4	98
Total	604	22	35	109	770

733

734

735 **Table 4: Cross-validation criteria for estimated flood quantiles by hydrological regions.**

Model	Criteria		1	2	3	4	5	6	7	All
GAM/TPS	NSH	Q10	84.8	86.4	92.8	89.6	81.1	90.8	74.7	94.7
		Q100	77.9	84.0	89.2	84.1	77.0	88.3	69.4	92.7
	MAD	Q10	0.236	0.267	0.237	0.344	0.375	0.325	0.252	0.298
		Q100	0.286	0.297	0.276	0.393	0.442	0.344	0.293	0.343
	ACV	Q10	0.063	0.069	0.061	0.057	0.141	0.099	0.067	0.090
		Q100	0.107	0.121	0.101	0.097	0.197	0.148	0.106	0.137
ROI/KRG	NSH	Q10	83.5	85.0	92.2	92.4	81.2	89.6	79.0	94.7
		Q100	77.2	80.3	89.6	87.9	76.2	88.0	73.2	92.7
	MAD	Q10	0.232	0.270	0.235	0.262	0.386	0.358	0.236	0.300
		Q100	0.279	0.334	0.250	0.334	0.439	0.368	0.281	0.340
	ACV	Q10	0.062	0.084	0.060	0.049	0.138	0.087	0.060	0.086
		Q100	0.107	0.137	0.102	0.086	0.202	0.123	0.096	0.133

736

737

*Bold indicates best of each criteria in column between models.

738

739
740
741

Table 5: Cross-validation criteria for estimated flood quantiles using different methods for evaluating the flood quantiles.

Model	Method	NSH		MAD	
		Q10	Q100	Q10	Q100
GAM/TPS	LRT	94.68	92.72	0.298	0.343
	IF	94.44	91.57	0.304	0.368
	IFW	94.43	91.73	0.304	0.365
	QRT	94.66	92.70	0.299	0.345
ROI/KRG	LRT	94.67	92.73	0.300	0.340
	IF	94.56	91.92	0.304	0.367
	IFW	94.53	92.03	0.305	0.363
	QRT	94.64	92.74	0.301	0.341

742
743
744
745

*Bold indicates best method in columns for each model.

746 **Table 6: Cross-validation criteria for estimated flood quantiles by provinces with**
 747 **(Provincial) and without (National) the use of administrative boundaries.**

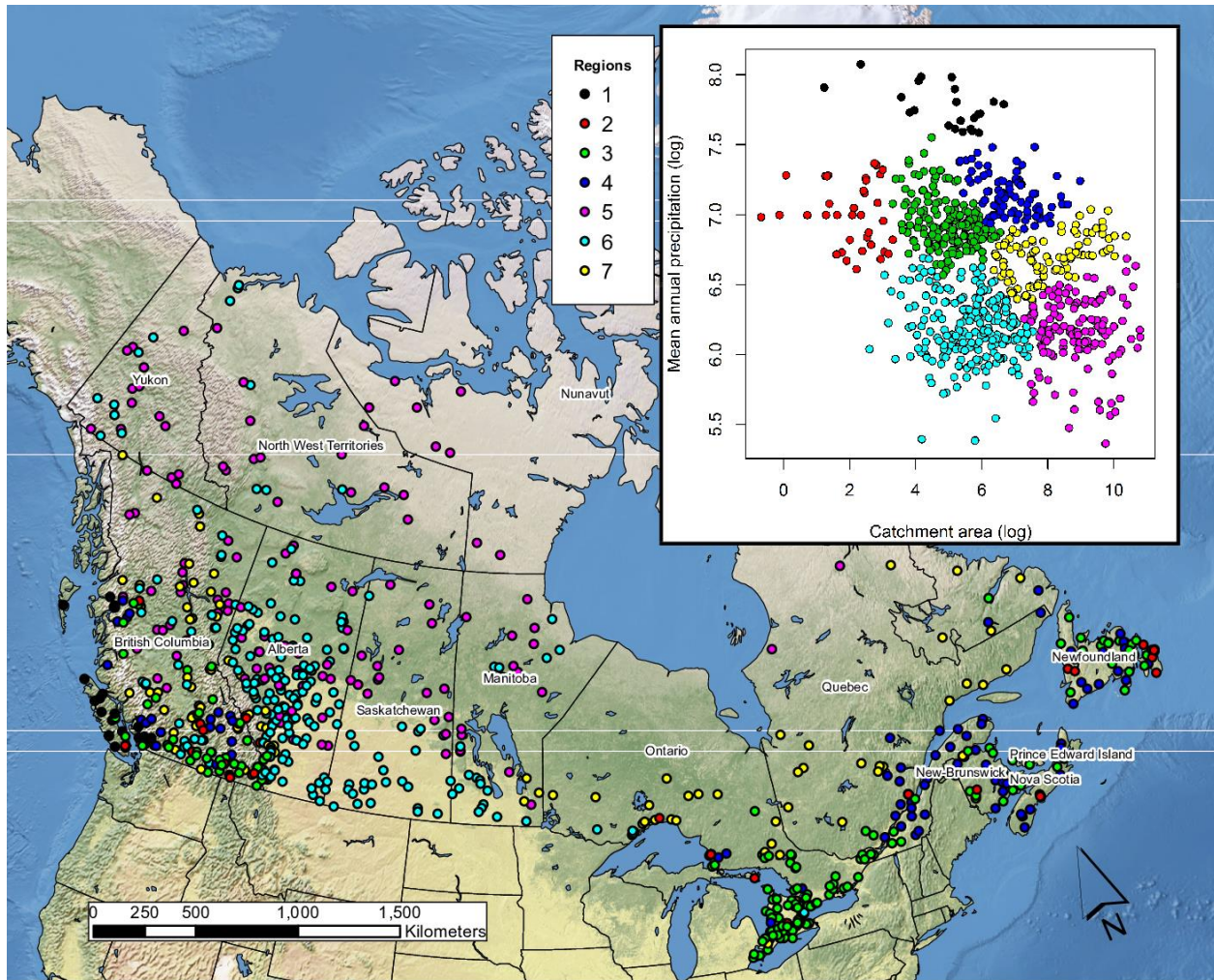
748

Model	Analysis			AB	ATL	BC	MS	NT	ON	QC	All
			nb. sites	177	83	192	81	51	128	58	770
GAM/TPS	National	NSH	Q10	90.2	96.0	95.5	86.0	94.2	93.3	97.5	94.7
			Q100	86.9	94.3	94.4	80.1	91.6	92.0	95.8	92.7
		MAD	Q10	0.353	0.227	0.296	0.360	0.338	0.251	0.228	0.298
			Q100	0.421	0.261	0.327	0.399	0.410	0.278	0.286	0.343
	Provincial	NSH	Q10	89.3	94.7	96.4	88.4	89.0	94.6	91.2	94.1
			Q100	85.6	93.6	95.2	79.8	86.3	93.6	86.0	91.6
		MAD	Q10	0.371	0.220	0.253	0.346	0.454	0.235	0.315	0.301
			Q100	0.424	0.269	0.291	0.418	0.505	0.264	0.393	0.350
ROI/KRG	National	NSH	Q10	91.2	95.9	95.6	86.3	90.4	94.5	96.3	94.7
			Q100	88.2	94.4	93.8	82.2	88.1	93.2	94.8	92.7
		MAD	Q10	0.35	0.209	0.277	0.382	0.431	0.237	0.267	0.300
			Q100	0.403	0.255	0.318	0.407	0.455	0.260	0.322	0.340
	Provincial	NSH	Q10	90.4	95.6	95.5	87.2	89.6	93.6	96.7	94.4
			Q100	87.4	93.5	93.9	81.6	86.0	92.7	95.2	92.3
		MAD	Q10	0.361	0.229	0.287	0.363	0.447	0.254	0.258	0.309
			Q100	0.406	0.268	0.332	0.406	0.509	0.275	0.305	0.350

749

750 * Bold indicates best criteria between national and provincial analysis for the same model.

751 **Figures**



752

753 **Figure 1: Locations of 770 hydrometric stations in Canada and descriptors space.**

754